Consequences of convection-radiation interaction for magnetite-water nanofluid flow due to a moving plate

Ammar Mushtaq [a], Junaid Ahmad Khan [a, 1], Meraj Mustafa [b], Tasawar Hayat [c, d] and Ahmed Alsaedi [d]

[a] *Research Centre for Modeling and Simulation (RCMS), National University of Sciences and Technology (NUST), Islamabad 44000, Pakistan*
[b] *School of Natural Sciences (SNS), National University of Sciences and Technology (NUST), Islamabad 44000, Pakistan*
[c] *Department of Mathematics, Quaid-I-Azam University 45320, Islamabad 44000, Pakistan*
[d] *Department of Mathematics, Faculty of Science, King Abdulaziz University, P. O. Box 80257, Jeddah 21589, Saudi Arabia*

Abstract: Present paper examines the boundary layer flow of magnetic nanofluid over a radiative plate moving in a uniform parallel free stream. Water is considered as the base fluid which is being filled with magnetite-Fe_3O_4 nanoparticles. Energy balance equation is formulated with non-linear radiation heat flux. Mathematical analysis is carried out through the famous Tiwari and Das model. Similarity approach is utilized to construct self-similar form of the governing differential system. Numerical computations are made through standard shooting method. Ferrofluid velocity is predicted to enhance upon increasing the nanoparticle volume fraction which contradicts with the available literature for non-magnetic nanofluids. It is found that Fe_3O_4-water ferrofluid has superior heat transfer coefficient than pure water. Results reveal that consideration of magnetic nanoparticles in water leads to better absorption of incident solar radiations. The well-known Blasius and Sakiadis flows are also explicitly analyzed from the present model.

Keywords: Ferrofluid; Heat transfer; Numerical treatment; Non-linear radiation; Blasius problem

[1]Corresponding author Tel.: + 92 333 4408815

E-mail address: tojunaidahmad@gmail.com

Nomenclature

(x, y)	2D Cartesian coordinate system (m)	$'$	1st order derivative with respect to η
u, v	velocity components along the $x-, y-$ directions (m/sec)	$''$	2nd order derivative with respect to η
T	fluid temperature (K)	$'''$	3rd order derivative with respect to η
T_w	wall temperature (K)	***Greek symbols***	
T_∞	ambient fluid temperature (K)	ν	kinematic viscosity (m^2/sec)
$B(x)$	magnetic field strength (N/(m·A))	α	thermal diffusivity (m^2/sec)
U	positive constant (m/sec)	η	similarity variable
c_p	specific heat (J/(Kg K))	λ	velocity ratio parameter
f	dimensionless $x-$ components of velocity	μ	dynamic viscosity (kg/m.sec)
C_f	skin friction coefficient	ϕ	nanoparticle volume fraction
Re	local Reynolds number	ρ	density (Kg/m^3)
Nu_x	local Nusselt number	τ_w	wall shear stress ($Kg/(m\ sec^2)$)
Ec	Eckert number	θ	dimensionless temperature
Rd	Radiation parameter	σ	electrical conductivity ($1/\Omega\,m$)
M	Hartman number	***Subscript***	
Pr	Prandtl number	s	nanoparticle material
q_r	Rosseland radiative heat flux respectively (W/m^2)	f	base fluid
k	thermal conductivity (W/(m·K))	nf	nanofluid
U_w, U_∞	velocity of the stretching sheet and far field respectively along $x-$ directions (m/sec)		

1. Introduction

Traditional sources of heat transfer liquids are incapable to deliver the modern cooling requirements primarily because of their weak convective heat transfer coefficients. Researches proved that nanoparticles, generally made of metals or oxides enhance conduction and convection coefficients and hence allow for rapid higher heat transfer rates out of the coolants. Thus heat transfer and efficiency of thermal systems can be improved via nanoparticle working fluid. Owing to their enhanced thermal conductivity, nanofluids have promising applications in several areas of industry and biomedicine. These include engine cooling, cooling of transformer oil, space and defense, electronics cooling, solar water heating, nuclear reactor cooling, refrigeration and many others. Detailed reviews about the possible heat transfer applications of nanofluids have been presented by Wang [1], Saidur et al. [2, 3], Mahian et al. [4] and Kasaeian et al. [5]. In the past, nanofluid flow and heat transfer due to moving or stationary surfaces have been given tremendous attention by the researchers [6-18]. Magnetic nanofluids, known as ferrofluids, are more beneficial than the ordinary nanofluids because their thermophysical properties can be amplified through external magnets. Ferrofluids possess a form of heat transfer known as thermo-magnetic convection which is beneficial when usual convection heat transfer is insufficient. Saharifi et al. [19] suggested using ferrite-based ferrofluids for drug delivery and hyperthermia treatment for cancer. Ferrofluids may serve to form liquid seals around the spinning drive shafts in hard disks. Some recent pertaining to the heat transfer characteristics of magnetic nanofluids can be seen through [20-24].

Study of radiative heat transfer has noteworthy importance in various branches of science and engineering. Raptis and Perdikis [25] investigated the radiation effects on viscoelastic fluid flow over a stationary heated plate. In this work, radiation term in the heat transfer equation was linearized through the assumption of negligible temperature differences within the flow. Later, such approximation has been adopted for investigating several other boundary layer flow problems even in recent past. Rahman and Eltayeb [26] firstly presented the heat transfer analysis through the exact expression of radiative heat flux. They investigated the flow of nanofluid bounded by a non-linearly stretching radiative surface. Blasius flow of viscous fluid with non-linear radiation was numerically explored by Pantokratoras and Fang [27]. Mushtaq et al. [28] viscous flow due to a bi-directional stretching surface subjected to non-linear radiation. Flow adjacent to a stationary vertical plate influenced by non-linear thermal radiation was investigated by Pantokratoras [29]. Mustafa et al. [30] studied the exponentially stretched flow in the existence of non-linear radiative heat flux. In another paper, flow of power-law fluid subject to non-linear radiation was studied by Mustafa et al. [31].

To our knowledge, the non-linear radiation effects in ferrofluid flow have never been reported previously. Therefore, present work aims to address the consequences of non-linear radiation heat flux in the boundary layer flow of Fe_3O_4-water ferrofluid due to constantly moving plate in parallel free stream. Such analysis even for non-magnetic nanofluids is not yet performed. Thermal conductivity of ferrofluid is estimated through the Maxwell model which is valid for spherical nanoparticles. Computational analysis is performed through the shooting method. Graphical illustrations for the effects of embedded physical parameters are presented and discussed in detail.

2. Model development

Consider a laminar flow of Fe_3O_4-water ferrofluid over a moving plate having constant velocity U_w. The plate is coincident with the plane $y=0$ while ferrofluid occupies the semi-infinite region $y \geq 0$. Let U_∞ be the free stream velocity. Flow is subjected to non-uniform magnetic field of strength $B(x)=B_0/\sqrt{x}$ in the transverse direction. The plate is kept at constant temperature T_w whereas T_∞ denotes the temperature at the far field. Thus relevant boundary layer equations governing the nanofluid flow and heat transfer with viscous dissipation and thermal radiation effects are expressed below (see [12] for details):

$$\frac{\partial u}{\partial x}+\frac{\partial v}{\partial y}=0, \tag{1}$$

$$\rho_{nf}\left(u\frac{\partial u}{\partial x}+v\frac{\partial u}{\partial y}\right)=\mu_{nf}\left(\frac{\partial^2 u}{\partial y^2}\right)-\sigma_{nf}B_0^{\,2}\left(u-U_\infty\right), \tag{2}$$

$$u\frac{\partial T}{\partial x}+v\frac{\partial T}{\partial y}=\alpha_{nf}\left(\frac{\partial^2 T}{\partial y^2}\right)-\frac{1}{\left(\rho c_p\right)_{nf}}\frac{\partial q_r}{\partial y}+\frac{\mu_{nf}}{\left(\rho c_p\right)_{nf}}\left(\frac{\partial u}{\partial y}\right)^2, \tag{3}$$

and the boundary conditions are:

$$u = U_w, \quad v = 0, \quad T = T_w \quad \text{at} \quad y = 0,$$
$$u \to U_\infty, \quad T \to T_\infty \quad \text{as} \quad y \to \infty. \tag{4}$$

In Eqs. (1)-(4), $u(x,y)$ and $v(x,y)$ denote the velocities along the $x-$and $y-$directions respectively, $q_r = -\left(4\sigma^* / 3k^*\right)\partial T^4 / \partial y$ is the radiation heat flux in which $\sigma^* = 8.61\times10^{-5}\,\text{eV/K}$ is the Boltzman constant and k^* is the mean absorption coefficient. Further the effective density ρ_{nf}, the effective viscosity μ_{nf}, the effective thermal diffusivity α_{nf}, the effective heat capacity $\left(\rho c_p\right)_{nf}$ and effective thermal conductivity k_{nf} are defined below:

$$\mu_{nf} = \frac{\mu_f}{(1-\phi)^{2.5}}, \qquad \alpha_{nf} = \frac{k_{nf}}{\left(\rho c_p\right)_{nf}}, \qquad \rho_{nf} = (1-\phi)\,\rho_f + \phi\rho_s, \tag{5}$$

$$\left(\rho c_p\right)_{nf} = (1-\phi)\left(\rho c_p\right)_f + \phi\left(\rho c_p\right)_s, \quad \frac{k_{nf}}{k_f} = \frac{\left(k_s + 2k_f\right) - 2\phi\left(k_f - k_s\right)}{\left(k_s + 2k_f\right) + \phi\left(k_f - k_s\right)}, \tag{6}$$

in which ϕ denotes the volume fraction of nanoparticles and subscripts s and f indicate solid and fluid phases respectively.

Electrical conductivity of nanofluid σ_{nf} is proposed by Maxwell [32] as

$$\frac{\sigma_{nf}}{\sigma_f} = \left[1 + \left\{\frac{3\left(\sigma_s - \sigma_f\right)\phi}{\left(\sigma_s + 2\sigma_f\right) - \left(\sigma_s - \sigma_f\right)\phi}\right\}\right]. \tag{7}$$

We consider the following transformations [6]:

$$\eta = y\sqrt{\frac{U}{2\nu_f x}}, \quad u = Uf'(\eta), \quad v = \sqrt{\frac{U\nu_f}{2x}}\left(\eta f' - f\right), \quad T = T_\infty + \left(T_w - T_\infty\right)\theta(\eta), \tag{8}$$

with $U = U_w + U_\infty$. In view of (8), Eq. (1) is satisfied and Eqs. (2)-(4) assume the following forms:

$$\frac{1}{(1-\phi)^{2.5}} f''' + \left(1 - \phi + \phi\rho_s / \rho_f\right) ff'' + M\,\frac{\sigma_{nf}}{\sigma_f}(\lambda - f') = 0, \tag{9}$$

$$\frac{1}{\Pr}\left(\left(k_{nf}/k_f+Rd\left(1+\left(\theta_w-1\right)\theta\right)^3\right)\theta'\right)'+\left(1-\phi+\phi\left(\rho c_p\right)_s/\left(\rho c_p\right)_f\right)f\theta' \\ +\frac{1}{\left(1-\phi\right)^{2.5}}Ecf''^2=0, \tag{10}$$

$$f\left(0\right)=0,\qquad f'\left(0\right)=1-\lambda,\quad \theta\left(0\right)=1, \\ f'\left(\infty\right)=\lambda,\qquad \theta\left(\infty\right)=0, \tag{11}$$

in which $\Pr=\left(\mu c\right)_f/k_f$ is the Prandtl number of pure water, $Rd=16\sigma^*T_\infty^{\ 3}/3k_fk^*$ the thermal radiation parameter, $M=\sigma B_0^2/\rho_fU$ the Hartman number, $Ec=U^2/c_p\left(T_w-T_\infty\right)$ the Eckert number and $\lambda=U_\infty/U$ the velocity ratio parameter. It is worth noting here that $M=0$ corresponds to the case of non-magnetic nanofluids which is not yet explored. Eqs. (8)-(10) correspond to the classical Blasius problem when $\lambda=1$ while Sakiadis flow problem is achieved by setting $\lambda=0$.

Skin friction coefficient C_f and the local Nusselt number Nu_x are defined as follows.

$$C_f=\frac{\tau_w}{\rho_fU^2},\ Nu_x=\frac{xq_w}{k_f(T_w-T_\infty)}, \tag{12}$$

where τ_w and q_w denote the wall shear stress and wall heat flux respectively. These are expressed as

$$\tau_w=\mu_{nf}\left.\frac{\partial u}{\partial y}\right|_{y=0},\ q_w=-k_{nf}\left.\frac{\partial T}{\partial y}\right|_{y=0}+q_r. \tag{13}$$

Invoking variables from Eq. (8) into Eq. (12) one obtains

$$\sqrt{\frac{Re_x}{2}}C_f=\frac{1}{(1-\phi)^{2.5}}f''(0),\ \frac{Nu_x}{\sqrt{2Re_x}}=-\left(k_{nf}/k_f+Rd\theta_w^3\right)\theta'(0), \tag{14}$$

where $Re_x=Ux/\nu_f$ is the local Reynolds number.

3. Numerical results and discussion

Nonlinear differential system given in Eqs. (9)-(11) has been evaluated numerically through standard shooting method with fifth-order Runge-Kutta integration and Newton's method. First of all we transformed Eqs. (8) and (9) into a system of first order equations by suitable substitutions: ($x_1 = f, x_2 = f', x_3 = f'', x_4 = \theta$ and $x_5 = \theta'$). We get

$$\begin{bmatrix} x_1' \\ x_2' \\ x_3' \\ x_4' \\ x_5' \end{bmatrix} = \begin{bmatrix} x_2 \\ x_3 \\ -\left(\left(1-\phi+\phi\left(\rho_s/\rho_f\right)\right)x_1x_3 + M\left(\sigma_{nf}/\sigma_f\right)\left(\lambda - x_2\right)\right)\left(1-\phi\right)^{2.5} \\ x_5 \\ -\dfrac{\begin{pmatrix} \Pr\left(1-\phi+\phi\left(\left(\rho c_p\right)_s/\left(\rho c_p\right)_f\right)\right)x_1x_5 + \left(\Pr Ec/\left(1-\phi\right)^{2.5}\right)x_3^2 \\ +3Rd\left(1+\left(\theta_w-1\right)x_4\right)^2\left(\theta_w-1\right)x_5^2 \end{pmatrix}}{\left(\left(k_{nf}/k_f\right)+Rd\left(1+\left(\theta_w-1\right)x_4\right)^3\right)} \end{bmatrix}, \tag{15}$$

subject to the following conditions

$$\begin{bmatrix} x_1 \\ x_2 \\ x_3 \\ x_4 \\ x_5 \end{bmatrix} = \begin{bmatrix} 0 \\ 1-\lambda \\ u_1 \\ 1 \\ u_2 \end{bmatrix}. \tag{16}$$

First order system (16) is then integrated numerically by RK5 through a suitable choice for $f''(0)$ and $\theta'(0)$. These values are refined by employing Newton's method until the solutions for f' and θ exponentially decay to zero with error tolerance less than 10^{-5}. The average CPU time for one set of outputs is around 1.5 sec.

In order to investigate the physical effects of embedded parameters on the solutions, we prepared the Figs. 1-8. Thermophysical properties of water and magnetite are listed in table 2. Fig. 1 gives the velocity distribution for different values of λ when $\phi = 0$ (pure water) and $\phi = 0.2$. Fluid flows faster above the plate when larger values of λ are accounted. The parameter λ compares the free stream velocity with the velocity of the plate. The variation in velocity with ϕ appears to be non-monotonic here.

Fig. 2 perceives the influence of Hartman number M on the velocity profile. The application of magnetic force in the y-direction gives resistance to the momentum transport due to which boundary layer thickness decreases. Similar variations in f' with M exist in Blasius and Sakiadis flows. In Blasius flow, the plate is at rest and only free stream velocity is present due to which there is inverted boundary layer structure. An increase in magnetic field parameter opposes the momentum transport due to which boundary layer thickness decreases. This can be observed through Fig. 2 in which velocity profiles move towards the wall when M is increased. The reduction in momentum boundary layer thickness accompanies with an increase in the velocity near the wall region.

In Fig. 3, we plot the skin friction coefficient $1/(1-\phi)^{2.5} f''(0)$ against the volume fraction ϕ in case of both Blasius and Sakiadis flow problems. As ϕ enlarges, there is almost a linear growth in skin friction coefficient for any given value of M. The magnitude of skin friction coefficient significantly rises when M is incremented.

Fig. 4 is presented to foresee the influence of volume fraction ϕ on the temperature profile. As expected, a growth in the nanoparticle volume fraction ϕ augments the temperature and the thickness of thermal boundary layer. Moreover temperature distribution in Sakiadis flow problem is larger in comparison to the Blasius flow problem.

Fig. 5 captures the behavior of temperature θ as the radiation parameter Rd varies from $Rd = 0$ to $Rd = 1$. Temperature θ rises sharply when Rd is increased. Temperature θ is also directly proportional to the Eckert number Ec. For sufficiently large values of Ec, an overshoot in temperature profiles near the wall is observed.

The influence of temperature ratio parameter θ_w on temperature distribution is sketched in Fig. 6. The parameter θ_w enhances the penetration depth of temperature function. In contrast to linear radiative heat transfer, here the energy balance equation involves thermal diffusivity of the form

$(\alpha_{nf} + 16\sigma^* T^3 / 3k^* k_{nf})$, which is temperature dependent. From this expression, it is evident that thermal boundary layer will be much thicker in the non-linear radiation case when compared with the linear radiation case. When θ_w is increased, the profiles become broader and take a special S-shaped form with an inflection point.

Fig. 7 gives the plot of local Nusselt number $Nu_x / \sqrt{2\,\mathrm{Re}_x}$ versus the volume fraction ϕ. The magnitude of local Nusselt number linearly increases with ϕ only when sufficiently stronger magnetic field strength is considered. Fig. 8 shows the local Nusselt number $Nu_x / \sqrt{2\,\mathrm{Re}_x}$ as a function of Prandtl number Pr at different values of Eckert number Ec. We observe that magnitude of $Nu_x / \sqrt{2\,\mathrm{Re}_x}$ has direct relationship with the Prandtl number Pr while it is inversely proportional to the Eckert number Ec.

Numerical results of local Nusselt number $Nu_x / \sqrt{2\,\mathrm{Re}_x}$ for different values of λ, θ_w and Rd are provided in table 2. Interestingly, a drastic rise in wall heat flux is observed when the velocity ratio parameter λ is varied from $\lambda = 0$ to $\lambda = 0.5$. Moreover both temperature ratio parameter θ_w and radiation parameter Rd support the heat transfer rate from the plate.

4. Concluding remarks

A numerical study for the boundary layer flow of magnetite-water ferrofluid over a constantly moving horizontal plate with parallel free stream is presented. Numerical results are derived by shooting method. The major aspects of this work are outlined below:

1. Skin friction coefficient in Fe_3O_4-water ferrofluid is much larger in comparison to pure water.
2. Different from the non-magnetic nanofluids, the velocity of the ferrofluid has non-monotonic relationship with ϕ.
3. Both magnetic field effect and free stream velocity serve to enhance convective heat transfer coefficient of ferrofluid.
4. The parameter λ has a dual behavior on the hydrodynamic boundary layer. When $\lambda = 1$, the velocity profile f' is a straight line.

5. Temperature θ and heat transfer rate from the plate are directly and non-linearly proportional to the radiation parameter Rd.
6. When wall to ambient temperature ratio (θ_w) is increased, temperature profile changes from normal shape to S-shaped form with a point of inflection.
7. The well-known Blasius and Sakiadis flow problems can be obtained as the special cases of present model.

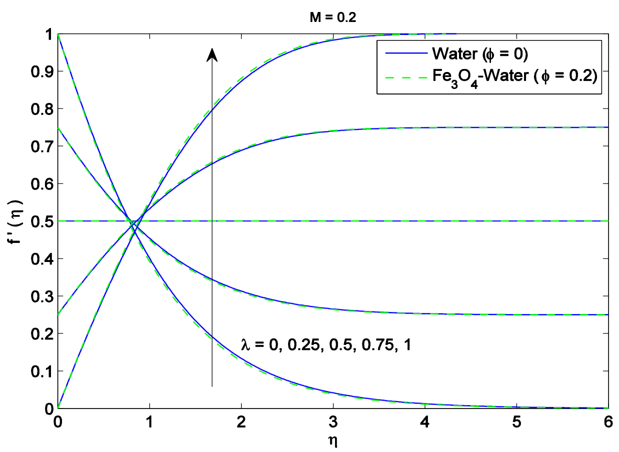

Fig. 1: Effect of λ on $f'(\eta)$.

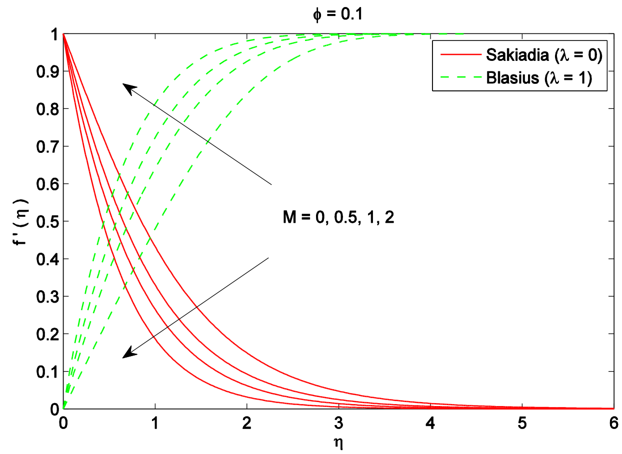

Fig. 2: Effect of M on $f'(\eta)$.

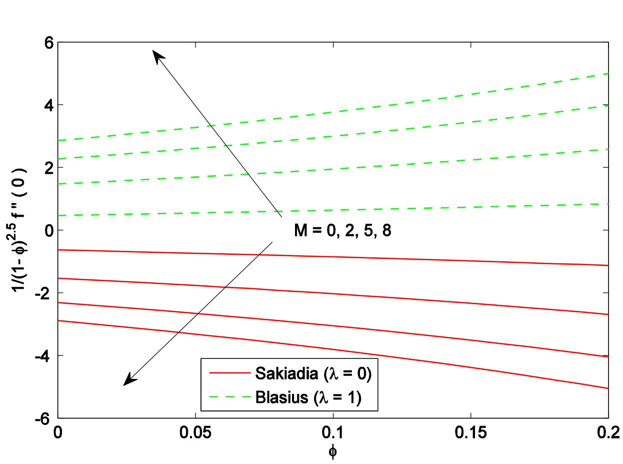

Fig. 3: Effect of λ, M and ϕ on Skin friction coefficient.

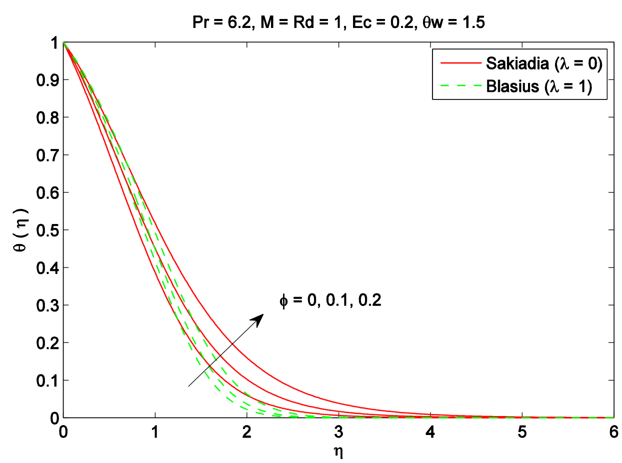

Fig. 4: Effect of ϕ on $\theta(\eta)$.

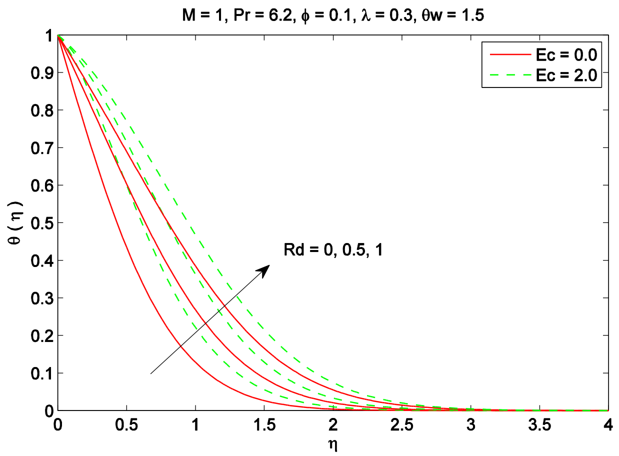

Fig. 5: Effect of Rd and Ec on $\theta(\eta)$.

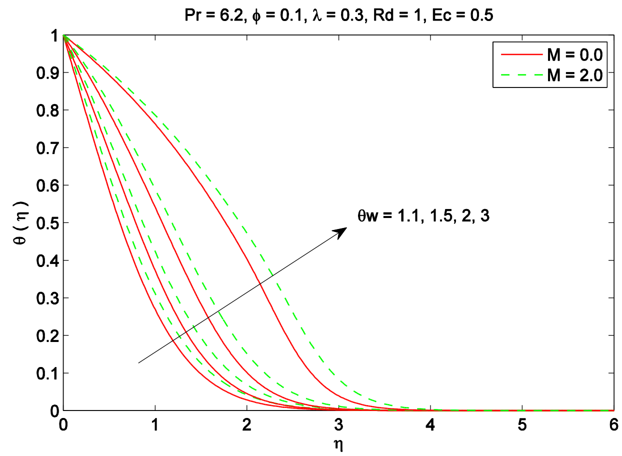

Fig. 6: Effect of M and θw on $\theta(\eta)$.

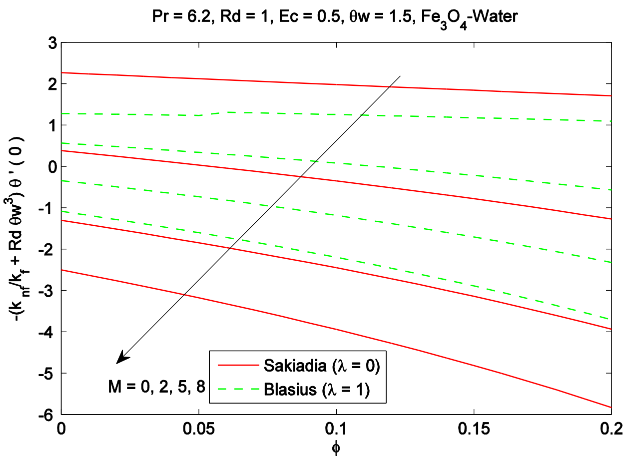

Fig. 7: Effect of λ, M and ϕ on Nusselt number.

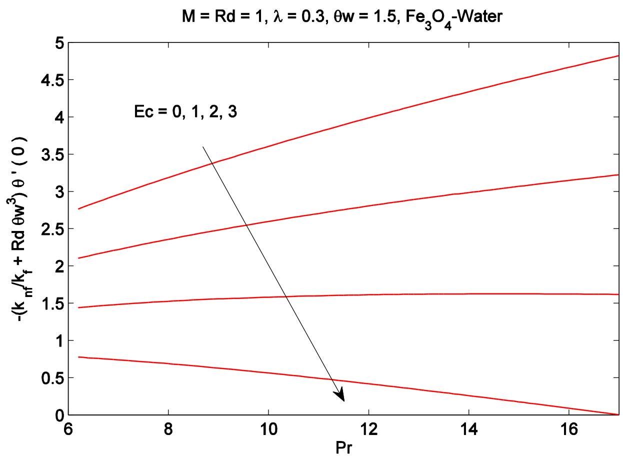

Fig. 8: Effect of Pr and Ec on Nusselt number.

Table 1: Thermo-physical properties of water and magnetite-Fe_3O_4.

	$\rho\left(\text{kg/m}^3\right)$	$c_p\left(\text{J/kg K}\right)$	$k\left(\text{W/mK}\right)$
Water	997.1	4179	0.613
Fe_3O_4	5180	670	9.7

References

1. X. Q. Wang and A. S. Mujumdar, A review on nanofluids-Part II, Brazilian J. Chem. Eng. 25 (2008) 631-648.

2. R. Saidur, K. Y. Leong and H. A. Mohammed, A review on applications and challenges of nanofluids, Renew. Sust. Ener. Rev. 15 (2011) 1646-1668.

3. R. Saidur, S. N. Kazi, M. S. Hossain, M. M. Rahman and H. A. Mohammed, A review on the performance of nanoparticles suspended with refrigerants and lubricating oils in refrigeration systems, Renew. Sust. Ener. Rev. 15 (2011) 310-323.

4. O. Mahian, A. Kianifar, S. A. Kalogirou, I. Pop and S. Wongwises, A review of the applications of nanofluids in solar energy, Int. J. Heat Mass Transf. 57 (2013) 582-594.

5. A. Kasaeian, A. T. Eshghi and M. Sameti, A review on the applications of nanofluids in solar energy systems, Renew. Sust. Ener. Rev. 43 (2015) 584-598.

6. D. A. Nield and A. V. Kuznetsov, Thermal instability in a porous medium layer saturated by a nanofluid: A revised model, Int. J. Heat Mass Transf. 68 (2014) 211-214.
7. A. V. Kuznetsov and D. A. Nield, Natural convective boundary-layer flow of a nanofluid past a vertical plate: A revised model, Int. J. Therm. Sci. 77 (2014) 126-129.
8. M. Turkyilmazoglu, Nanofluid flow and heat transfer due to a rotating disk, Comp. Fluids 94 (2014) 139-146.
9. M. M. Rashidi, S. Abelman and N. F. Mehr, Entropy generation in steady MHD flow due to a rotating porous disk in a nanofluid, Int. J. Heat Mass Transf. 62 (2013) 515-525.

10. M. Sheikholeslami, F. B. Sheykholeslami, S. Khoshhal, H. Mole-Abasia, D. D. Ganji and H. B. Rokni, Effect of magnetic field on Cu–water nanofluid heat transfer using GMDH-type neural network, Neural Comput. Appl. 25 (2014) 171-178.
11. A. Malvandi and D. D. Ganji, Magnetic field effect on nanoparticles migration and heat transfer of water/alumina nanofluid in a channel, J. Magnet. Magn. Mater. 362 (2014) 172-179.
12. A. Mushtaq, M. Mustafa, T. Hayat and A. Alsaedi, Nonlinear radiative heat transfer in the flow of nanofluid due to solar energy: A numerical study, J. Taiwan Inst. Chem. Eng. 45 (2014) 1176-1183.
13. M. M. Rashidi, N. Freidoonimehr, A. Hosseini, O. A. Bég and T. K. Hung, Homotopy simulation of nanofluid dynamics from a non-linearly stretching isothermal permeable sheet with transpiration, Meccan. 49 (2014) 469-482.
14. D. A. Nield and A. V. Kuznetsov, Forced convection in a parallel-plate channel occupied by a nanofluid or a porous medium saturated by a nanofluid, Int. J. Heat Mass Transf. 70 (2014) 430-433.
15. M. Mustafa and J. A. Khan, Model for flow of Cassonnanofluid past a non-linearly stretching sheet considering magnetic field effects, AIP Adv. doi: 10. 1063/1.4927449.
16. J. A. Khan, M. Mustafa, T. Hayat and A. Alsaedi, Three-dimensional flow of nanofluid over a non-linearly stretching sheet: An application to solar energy, Int. J. Heat Mass Transf. 86 (2015) 158-164.
17. J. A. Khan, M. Mustafa, T. Hayat, M. Sheikholeslami and A. Alsaedi, Three-dimensional flow of nanofluid induced by an exponentially stretching sheet: An application to solar energy, PLoS ONE 10 (2015) doi:10.1371/journal.pone.0116603.
18. M. Mustafa, J. A. Khan, T. Hayat and A. Alsaedi, On Bödewadt flow and heat transfer of nanofluids over a stretching stationary disk. J. Mol. Liq. 211 (2015) 119-125.
19. I. Sharifi, H. Shokrollahi and S. Amiri, Ferrite based magnetic nanofluids used in hyperthermia applications, J. Magnet. Magn. Mater. 324 (2011) 903-915.
20. H. Aminfar, M. Mohammadpourfard and F. Mohseni, Two-phase mixture model simulation of the hydro-thermal behavior of an electrical conductive ferrofluid in the presence of magnetic fields, J. Magn. Magn. Mater. 324 (2012) 830–842.

21. F. Selimefendigil and H. F. Oztop, Effect of a rotating cylinder in forced convection of ferrofluid over a backward facing step, Int. J. Heat Mass Transf. 71 (2014) 142–148.
22. M. Sheikholeslami, M. Gorji-Bandpy, R. Ellahi and A. Zeeshan, Simulation of MHD CuO–water nanofluid flow and convective heat transfer considering Lorentz forces, J. Magn. Magn. Mater. 369 (2014) 69–80
23. A. Malvandi and D. D. Ganji, Magnetic field effect on nanoparticles migration and heat transfer of water/alumina nanofluid in a channel, J. Magn. Magn. Mater. 362 (2014) 172-179.
24. X. Zhang and H. Huang, Effect of magnetic obstacle on fluid flow and heat transfer in a rectangular duct, Int. Commun. Heat Mass Transf. 51 (2014) 31–38.
25. A. Rapits and C. Perdikis, Viscoelastic flow by the presence of radiation, ZAMP 78 (1998) 277–279.
26. M. A. Seddeek, Effects of radiation and variable viscosity on MHD free convection flow past a semi infinite flat plate with an aligned magnetic field in the case of unsteady flow, Int. J. Heat Mass Transf. 45 (2002) 931–935.
27. A. Pantokratoras and T. Fang, Blasius flow with non-linear Rosseland thermal radiation, Meccan. 49 (2014) 1539-1545.
28. A. Mushtaq, M. Mustafa, T. Hayat and A. Alsaedi, On the numerical solution of the nonlinear radiation heat transfer in a three-dimensional flow, Z. Naturforsch. 69a (2014) 705-713.
29. A. Pantokratoras, Natural convection along a vertical isothermal plate with linear and non-linear Rosseland thermal radiation, Int. J. Therm. Sci. 84 (2014) 51-57.
30. M. Mustafa, A. Mushtaq, T. Hayat and A. Alsaedi, Radiation effects in three-dimensional flow over a bi-directional exponentially stretching sheet, J. Taiwan Inst. Chem. Eng. 47 (2015) 43-49.
31. M. Mustafa, A. Mushtaq, T. Hayat and A. Alsaedi, Model to study the non-linear radiation heat transfer in the stagnation-point flow of power-law fluid, Int. J. Num. Meth. Heat & Fluid Flow 25 (2015) 1107-1119.
32. J. C. Maxwell, A treatise on electricity and magnetism, 2nd Ed. Cambridge: Oxford University Press; 1904. pp. 435-41.

Table 2: Numerical values of local Nusselt number $Nu_x / \sqrt{2\,\mathrm{Re}_x}$ when $M = 1, Pr = 6.2, Ec = 0.5$ and $\phi = 0.2$.

λ	θ_w	Rd	$-\left(k_{nf} / k_f + Rd\theta w^3\right)\theta'(0)$
0	1.5	1	-0.0062596954
0.2			1.9233832
0.5			2.8784479
1			0.17352702
0.5	1.1		2.4715736
	1.5		2.8785745
	2		3.5724593
	2.5		4.3961313
	1.5	0	1.9517906
		0.5	2.4641607
		1	2.8785745
		1.5	3.2432484

Paper submitted: November 27, 2015
Paper revised: July 26, 2016
Paper accepted: July 27, 2016